PHYSICAL REVIEW B VOLUME 57, NUMBER 8 15 FEBRUARY 1998-II

Effect of nonequilibrium LO phonons and hot electrons on far-infrared intraband absorption in *n*-type GaAs

H. P. M. Pellemans
Department of Applied Physics, Delft University of Technology, P.O. Box 5046, 2600 GA Delft, The Netherlands

P. C. M. Planken*
FOM-Institute for Plasmaphysics ''Rijnhuizen,'' 3430 BE Nieuwegein, The Netherlands

(Received 7 August 1997)

We report far-infrared transient-grating measurements in *n*-type GaAs in which we observe that nonequilibrium longitudinal-optical (LO) phonons, emitted by hot electrons, directly couple in the infrared ($\sim 17\ \mu$m) intraband absorption process. We find that a few picoseconds after the far-infrared optical excitation, the time evolution of the induced intraband absorption change is in fact completely dominated by these nonequilibrium phonons. This observation is possible because *intra*band absorption, contrary to optical *inter*band absorption, is a second-order *LO-phonon-assisted* process, which is directly affected by changes in both the electron distribution *and* the LO-phonon distribution. [S0163-1829(98)51408-7]

Intraband absorption of light in *n*-type doped polar semiconductors such as GaAs is the net difference between photon-induced electronic transitions from lower to higher, or from higher to lower conduction-band states under the simultaneous emission or absorption of longitudinal-optical (LO) phonons [Fig. 1(a)].[1,2] Very little is known about intraband absorption under conditions when the electron gas, the LO phonons, and the other lattice modes are not equilibrated with each other. Experiments in the past have shown that such a nonequilibrium situation can arise in *inter*band experiments when an ultrashort visible laser pulse excites electron-hole pairs across the band gap of a semiconductor. This gives rise to a hot-electron distribution in the conduction band of the semiconductor, which cools mainly by emitting LO phonons. These changes in the electron distribution can be studied by monitoring, for example, luminescence from interband recombination of electron-hole pairs.[3] Changes in the LO-phonon distribution have been observed directly with time-resolved Raman-scattering measurements,[4] or indirectly by the effect they have on the electron distribution, such as a reduction of the electron-gas cooling rate.[5–9]

At present little is known about the effect of hot electrons and nonequilibrium phonons on the intraband absorption process due to the lack of suitable mid/far-infrared laser sources. Such a source is necessary to excite electrons within the conduction band without creating additional electron-hole pairs through single- or multi-photon interband excitation. In the past, time-resolved intraband pump-probe measurements in highly doped *n*-type InAs showed some evidence for the presence of nonequilibrium phonons influencing the intraband absorption dynamics.[10,11] That experiment demonstrated how nonequilibrium phonons are reabsorbed by the electron gas, the so-called hot-phonon effect, thus reducing the electron cooling rate and the decay of the corresponding intraband absorption change. These experiments, however, had a time resolution determined by the relatively long laser pulses of 8 ps duration and were limited to wavelengths below 9.5 μm.

Here, using subpicosecond pulses with a wavelength around 17 μm, we show the dramatic effect that hot electrons and nonequilibrium phonons have on the intraband absorption dynamics in GaAs. In the experiment, a far-IR pump pair creates a hot-electron distribution in *n*-type GaAs that gives rise to an initial intraband-absorption change. The

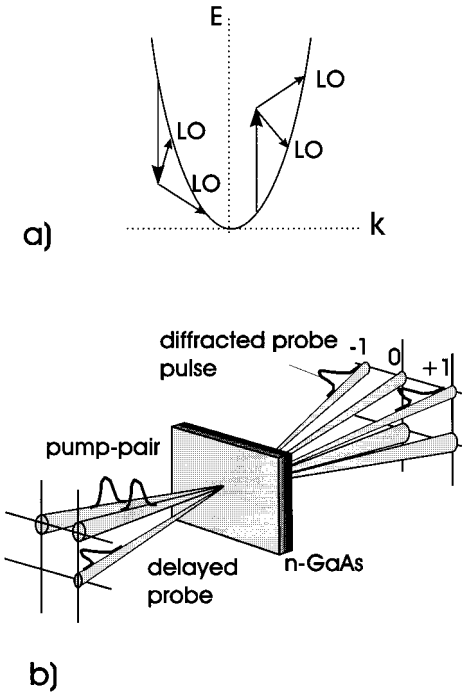

FIG. 1. (a) Schematic picture of the conduction band with energy vs wave vector of the electrons. The four possible LO-phonon assisted intraband transitions are shown. The vertical arrows correspond to the optical wave vectors of the mid/far-infrared light. (b) Geometry of the three-pulse transient-grating setup. The polarization of the probe beam is rotated 90° with respect to that of the pump pair. The diffracted probe beam is spatially separated from the pump pair after the focus.

decay of this change is monitored by diffracting a third delayed probe pulse off the grating. From a comparison with model calculations we find that nonequilibrium phonons, generated by the cooling electron gas, are reabsorbed by the electrons and thus reduce the cooling rate and, consequently, stretch the time evolution of the absorption change. More importantly, at the wavelengths used in our experiment ($\sim 17\ \mu$m), nonequilibrium LO phonons *directly couple in the LO-phonon-assisted absorption process* and *induce an additional, large, absorption change*. This mechanism greatly enhances the pump-induced absorption change and is essential in explaining the dynamics of the intraband absorption coefficient. This is even true when, at low excitation intensities, the cooling of the electron gas gives rise to relatively small changes of the LO-phonon occupation number. Our measurements clearly show that long-wavelength mid/far-IR pulses are *directly* sensitive to the nonequilibrium LO-phonon dynamics, even though LO phonons themselves are not infrared active.

Our sample is a (100)-oriented GaAs wafer with an electron concentration of 3.3×10^{17} cm^{-3}. The sample is polished on both sides, has a thickness of 0.12 mm, and is kept at a temperature of 300 K. The experimental setup uses pulses from the free-electron laser FELIX in the Netherlands.[12] This laser generates trains of pulses of 5 μs duration, in which the time separation between the pulses is 40 ns. The pulse trains emerge from the laser at a 5 Hz repetition rate. The laser is tunable from 5 to 110 μm and delivers pulse energies of up to 50 μJ. Pulse durations range from 0.35 ps at 9 μm to 0.55 ps at 17 μm and 0.7 ps at 20.5 μm as measured by standard second-harmonic autocorrelation measurements in CdTe. The pulses pass through an adjustable wire-grid attenuator that can attenuate the beam in discrete steps. Using a paraboloidal mirror, two intense pump pulses with spatial and temporal overlap are focused onto the sample and form an excitation grating. Using mirrors, we rotate the polarization of a third split-off pulse by 90° with respect to the pump-pair polarization, to minimize coherent coupling between the probe beam and the pump pair in the sample. After passing through another wire-grid attenuator, the probe pulse then undergoes a variable delay and is focused onto the same spot on the sample as the pump pair [Fig. 1(b)]. In the experiment, we detect the first-order diffracted probe beam as a function of the time delay between the pump pair and the probe, using a liquid-nitrogen cooled $Hg_{1-x}Cd_xTe$ detector.

The main results of our measurements are shown in Fig. 2 (solid lines), where we plot the normalized first-order diffracted probe signal vs pump-pair/probe time delay for seven different excitation intensities, when the laser is tuned to a wavelength of 17 μm. Normalization is obtained when the points that make up each curve are divided by the maximum value reached in that curve. For low excitation intensities, the diffracted signal reaches a maximum around time-delay zero when the pump pair and the probe have perfect temporal overlap. For positive time delays, the diffracted signal decreases and disappears on a time scale of approximately 4 ps. Remarkably, however, when we increase the excitation intensity, the diffracted signal no longer peaks at delay zero. Instead, the maximum in the diffracted signal shifts to longer delays and only a small shoulder remains around delay zero.

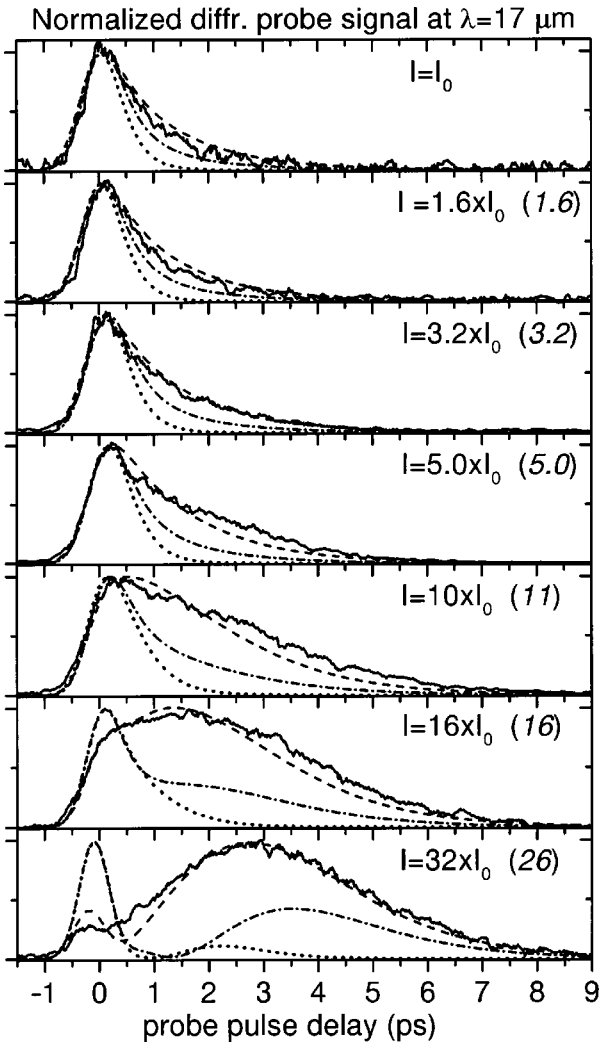

FIG. 2. Measured and calculated diffracted probe signals in n-type GaAs for seven different intensities. The intensity is indicated by the factor relative to the intensity used in the topmost picture. Three numerically calculated curves are shown in each plot. The intensity used in the calculations is indicated by a factor (in parentheses) relative to the intensity used in the calculation of the topmost figure. The dash-dotted curve is a calculation using identical parameters as in the full calculation but with the coupling of the nonequilibrium phonons in the optical intraband transitions turned off. The dashed curve represents the full calculation as described in the text. The dotted line is a calculation using identical parameters but with all nonequilibrium phonon effects turned off.

In addition to this, the apparent decay becomes somewhat slower and the diffraction now disappears after approximately 8 ps. We stress that these results were obtained in doped n-type GaAs samples with a constant carrier density and that we were unable to measure these effects in undoped samples. The highest diffraction efficiency that we observed is approximately $\sim10^{-2}$.

The origin of the diffracted probe signals cannot be explained on the basis of changes in the electron distribution alone. In fact, as we will discuss below, excitation of the n-type GaAs sample with an infrared pump pulse induces changes in the electron distribution *and* the LO-phonon distribution and *both* give rise to changes in the intraband absorption coefficient. To confirm that this interpretation is cor-

rect and to elucidate the effect that nonequilibrium phonons have on the intraband absorption, we have calculated the time-dependent intraband absorption coefficient $\alpha(t)$ taking the dynamics of the electrons and the LO phonons, generated by the cooling electrons, into account. From the absorption coefficient, we can calculate the diffraction efficiency, which is proportional to $|\alpha(t)-\alpha(t=-\infty)|^2$. We then convolute this with the probe-pulse shape to obtain the diffracted signal. In our calculations,[13] shown as the dashed lines in Fig. 2, we adjust the excitation intensity until good agreement is obtained with one of the measured curves. For the top measurement in Fig. 2, the best agreement is obtained for $I_0 = 14\ \mathrm{MW/cm^2}$, which compares well with the experimentally estimated intensity. It is important to realize that the value of the intensity thus obtained also determines the intensities that correspond with the remaining curves in Fig. 2. This is because in the experiment, the calibration of the attenuation *factor* is good even though the accuracy of the *absolute* intensity measurements is poor. Using this same attenuation factor in our calculations, we now find that we reproduce most of the remaining probe diffraction curves shown in Fig. 2, obtained at different pump intensities. An exception is formed by the fifth and the seventh curve, for which we had to assume a somewhat higher intensity, $11\times I_0$, instead of $10\times I_0$, and a somewhat lower intensity, $26\times I_0$, instead of $32\times I_0$, respectively, with I_0 the lowest intensity used. The former difference could be traced back to a temporary increase in the average output power of the laser during this particular measurement. The latter difference has another explanation as we will discuss below.

It is important to realize that the diffraction efficiencies $\eta=I_{\mathrm{Diffr}}/I_{in}=(\Delta\alpha d/4)^2$,[14] obtained using the calculated values of the absorption changes $\Delta\alpha$, with d the thickness of the sample, are not large enough to explain the measured maximum efficiencies of $\eta\sim10^{-2}$. This discrepancy is caused by the fact that the observed diffraction is in fact dominated by refractive-index changes instead of absorption changes. This is supported by calculations of the refractive-index change using a Kramers-Kronig transformation of the calculated absorption for a broad wavelength range. These calculations show that the induced absorption and refractive-index change are linearly proportional at 17 μm (to within a few percent). As both the experimental and the calculated curves in Fig. 2 are normalized, it therefore suffices to plot the calculated curves using the calculated absorption changes at this particular wavelength only.

The good agreement between the experimental results and the calculations allows us to use our calculations to selectively study the various contributions to the intraband absorption change. First, to emphasize that nonequilibrium LO phonons dominate the dynamics of the intraband absorption, we show in Fig. 2 calculations (dotted lines) of the diffracted signal in which the LO-phonon dynamics is turned off. It is clear that these calculations completely fail in reproducing both the shape of the measured diffraction and the time scale at which the diffracted signal disappears. This is because nonequilibrium phonons, generated by the cooling of the electron gas, profoundly influence the intraband absorption process in two ways. First, they can be reabsorbed by the electrons, thus reducing the cooling speed of the electron gas and the corresponding decay of the pump-induced absorption change. Second, they directly couple in the intraband absorption process, which is a LO-phonon-assisted process. The reduction in the cooling speed of an electron gas has been observed in the past in studies using visible pulses, and is known as the hot-phonon effect.[4–9,15] In Fig. 2 we have plotted the calculated diffracted signal (dash-dotted lines) when this hot-phonon effect is taken into account. Although the time decay thus calculated is slower than the time decay calculated when the LO-phonon dynamics is completely turned off, the calculations still fail in reproducing the measurements. This is because the largest nonequilibrium phonon contribution to the intraband absorption change is not the hot-phonon effect but *the direct coupling of nonequilibrium phonons in the intraband absorption process*. Only when we additionally include this effect in the calculations do we obtain the good agreement with our experimental results already shown in Fig. 2 by the dashed lines. The effect on the intraband absorption at 17 μm is so strong because the range of phonon wave vectors generated by the cooling electrons overlaps strongly with the range of wave vectors of the LO phonons taking part in the intraband absorption. This remarkable direct dependence of the intraband absorption change on the presence of nonequilibrium LO phonons contrasts strongly with *inter*band absorption or emission processes, which are not LO-phonon assisted processes in GaAs.

Our calculations include the effects of electron scattering between the Γ valley and the L valleys. When electrons scatter to the L valley, this decreases the Γ valley intraband absorption because fewer carriers are available to absorb light. This absorption decrease, however, is overwhelmed by the absorption increase caused by the growing number of nonequilibrium phonons generated by cooling electrons. Absorption of light by carriers in the L valley is not included in the calculations. This is because for most intensities the fraction of electrons present in the L valleys remains small. In addition, the effective electron mass in the L valley is much higher than in the Γ valley, giving rise to a smaller absorption coefficient. The largest fraction of electrons in the L valley, 10%, is obtained for the highest excitation intensity and for a pump-pair/probe delay of approximately 1 ps. It is probable then that the optical absorption by L-valley electrons can no longer be neglected. This could explain why the intensity used in the calculation to obtain a good agreement with the experimentally measured curve obtained at the highest excitation intensity is somewhat lower than the experimental value. An approximate calculation, in which we treat the L-valley absorption as arising from four spherical parabolic valleys with identical density-of-states effective electron masses, shows that this will shift the apparent diffraction maximum to smaller delays. This is because the largest contribution of the L-valley electrons to the absorption change occurs for small delays. The intensity now needed in the calculations to shift this maximum to longer delays again will more closely resemble the expected value. Such a calculation gives us a qualitative understanding of the effects of L-valley electrons on the total intraband absorption signal. A more realistic model would have to take the ellipsoidal nature of the L valleys into account. For the most part, however, the L valleys essentially serve as a small reservoir of electrons that scatter back to the Γ valley. At high intensities,

the largest effect of intervalley scattering is then to make the overall decay of the diffracted curves for delays larger than 3 ps somewhat slower.

When the electron gas cools, the LO-phonon occupation number increases and reaches a maximum a few picoseconds after optical excitation with the pump pulse. The time delay after optical excitation at which this maximum occurs increases when the optical intensity is increased, because it takes longer for the electron gas to cool down. As outlined above, at the optical wavelengths employed in our experiment, the nonequilibrium phonons dominate the intraband absorption change. To a great extent, this explains why the measured diffracted signals roughly peak for time delays when the phonon occupation numbers reach a maximum and not for time delays around zero, as evidenced by the results shown in Fig. 2.

At low intensities, the changes in the electron temperature and the LO-phonon distribution are small, but the nonequilibrium phonons still dominate the absorption *change*. In a sense, the electrons act as probes to optically detect the presence of nonequilibrium LO phonons, which are themselves not infrared active.

In conclusion, we have shown that nonequilibrium phonons in GaAs generated by cooling electrons completely dominate the pump-induced infrared intraband absorption change. First, they reduce the cooling speed of the electron gas and, second, they directly couple in the intraband absorption process.

We would very much like to thank Professor Dr. W. Th. Wenckebach and Dr. H. J. Bakker for useful discussions and for carefully reading the manuscript. We gratefully acknowledge the skillful assistance by the FELIX staff, in particular Dr. A. F. G. van der Meer. This work was performed as part of the research program of the Stichting voor Fundamenteel Onderzoek der Materie (FOM) with financial support from the Nederlandse Organisatie voor Wetenschappelijk Onderzoek (NWO).

---

*FAX: +31 30 6031204. Electronic address: planken@rijnh.nl

[1] B. K. Ridley, *Quantum Processes in Semiconductors*, 3rd ed. (Oxford Science, Clarendon, Oxford, 1993).

[2] K. Seeger, *Semiconductor Physics*, 5th ed. (Springer, Berlin, 1990).

[3] J. Shah, B. Deveaud, T. C. Damen, W. T. Tsang, A. C. Gossard, and P. Lugli, Phys. Rev. Lett. **59**, 2222 (1987).

[4] K. T. Tsen, R. P. Joshi, D. K. Ferry, and H. Morkoc, Phys. Rev. B **39**, 1446 (1989).

[5] Jagdeep Shah, *Ultrafast Spectroscopy of Semiconductors and Semiconductor Nanostructures* (Springer, Berlin, 1996).

[6] P. Kocevar, Physica **134B**, 155 (1985).

[7] W. Cai, M. C. Marchetti, and M. Lax, Phys. Rev. B **35**, 1369 (1987).

[8] X. Q. Zhou, H. M. van Driel, W. W. Rühle, and K. Ploog, Phys. Rev. B **46**, 16 148 (1992).

[9] S. S. Prabhu, A. S. Vengurlekar, S. K. Roy, and J. Shah, Phys. Rev. B **51**, 14 233 (1995).

[10] T. Elsaesser, R. J. Bäuerle, and W. Kaiser, Phys. Rev. B **40**, 2976 (1989).

[11] R. J. Bäuerle, T. Elsaesser, and W. Kaiser, Semicond. Sci. Technol. **5**, S176 (1990).

[12] D. Oepts, A. F. G. van der Meer, and P. W. van Amersfoort, Infrared Phys. Technol. **36**, 297 (1995).

[13] Our calculations are similar to the calculations presented in Ref. 1. Starting from second-order perturbation theory, rate equations are derived for the intraband absorption/emission rates. Starting from first-order perturbation theory, rate equations are derived for intervalley scattering and LO-phonon absorption and emission. The calculations incorporate static screening, possible degeneracy of the electron gas, and assume that the conduction band is parabolic and that the electron distribution is a Fermi distribution. All required material parameters of GaAs, like the effective electron masses, dielectric constants, and intervalley deformation potential are known and can be found in the literature. We used an LO-phonon lifetime of 2 ps, a value published by F. Vallée, Phys. Rev. B **49**, 2460 (1994). Details of the calculations will be published elsewhere.

[14] H. J. Eichler, P. Günter, and D. W. Pohl, *Laser-Induced Dynamic Gratings* (Springer, Berlin, 1986).

[15] W. Pötz and P. Kocevar, Phys. Rev. B **28**, 7040 (1983).